

Maja Stanisavljevic¹
Jana Chomoucka²
Simona Dostalova¹
Sona Krizkova^{1,2}
Marketa Vaculovicova^{1,2}
Vojtech Adam^{1,2}
Rene Kizek^{1,2}

¹Department of Chemistry and Biochemistry, Faculty of Agronomy, Mendel University in Brno, Zemedelska, Czech Republic

²Central European Institute of Technology, Brno University of Technology, Technicka, Czech Republic

Received April 16, 2014

Revised June 12, 2014

Accepted June 18, 2014

Research Article

Interactions between CdTe quantum dots and DNA revealed by capillary electrophoresis with laser-induced fluorescence detection

Quantum dots (QDs) are one of the most promising nanomaterials, due to their size-dependent characteristics as well as easily controllable size during the synthesis process. They are promising label material and their interaction with biomolecules is of great interest for science. In this study, CdTe QDs were synthesized under optimal conditions for 2 nm size. Characterization and verification of QDs synthesis procedure were done by fluorimetric method and with CE. Afterwards, QDs interaction with chicken genomic DNA and 500 bp DNA fragment was observed employing CE-LIF and gel electrophoresis. Performed interaction relies on possible matching between size of QDs and major groove of the DNA, which is approximately 2.1 nm.

Keywords:

Bacteriophage / DNA / Interaction / Quantum dots

DOI 10.1002/elps.201400204

1 Introduction

Nanoscale materials with very good electronic, optical, magnetic, and catalytic properties have made nanotechnology one of the most perspective scientific fields today. Quantum dots (QDs) belong to a large family of nanoparticles attracting enormous attention especially due to the small size and size-dependent characteristics. With their size (1–20 nm) they do not obey rules of classical physics and they belong to unpredictable laws of quantum mechanics. Precisely, their optical and electronic properties are caused by phenomena called quantum confinement [1]. Wide absorbance band, narrow emission spectrum, and/or photostability are well-known properties of QDs, which made them the most promising substitute for organic dyes. Another advantage of these materials is their ability to be easily modified, which is primarily done to decrease potential danger of inorganic core toxicity, but these surface modification can be also done to target some biomolecules and, thus, to image biochemical pathways in vivo. Beside their successful application in in vivo imaging [2–5] and/or biology [6] in general, their applications into proteomics gain more and more attention [7–10]. Moreover, currently a great attention is paid to the targeted drug/gene delivery and the combination of therapeutic and diagnostic

properties of various bioconjugates is explored, QDs are an excellent option for fluorescent labeling of numerous delivery systems. Not only a range of modern artificial nanomaterials but also traditionally utilized viral-based nanocarriers such as bacteriophages belong among such nanocarriers employed for targeted delivery [11]. In the case of nucleic acids delivery, revolutionary discovery of DNA structure done by Watson and Crick in 1953 [12] opened numerous challenges in this field of research. Rapid growth of nanomaterials such as QDs induced their inevitable encounter with DNA. Possible interaction between DNA and other molecules or species is provided by electrostatic binding in major groove of dsDNA and intercalation between base pairs [13]. Investigation of QDs and DNA have not been only directed to their interaction [14], but QDs have been successfully functionalized by DNA and used for fluorescence monitoring in vivo or in vitro [15, 16].

CE-LIF is a very powerful method for analysis of different nanoparticles in size, shape, or due to their charge [17–19]. QDs have been successfully characterized by CE-LIF [17, 20, 21], which have been also applied for separation and characterization of biomolecules labeled with QDs as a fluorescent marker [5, 22–25]. For biological application of QDs, their conjugation to biomolecules is an ongoing problematic and research challenge. The overview of advances can be found in various review articles [26–28].

Based on aforementioned knowledge, CE-LIF was chosen as a suitable method for monitoring of interaction between QDs and DNA depending on the concentration, time of interaction, length of the DNA strand, and/or its form (ssDNA

Correspondence: Dr. Rene Kizek, Department of Chemistry and Biochemistry, Mendel University in Brno, Zemedelska 1, CZ-613 00 Brno, Czech Republic

E-mail: kizek@sci.muni.cz

Fax: +420-5-4521-2044

Abbreviations: GSH, glutathione; QD, quantum dot

Colour Online: See the article online to view Figs. 1–5 in colour.

vs. dsDNA). This method can be used for a very simple DNA labeling with QDs and/or observing possible toxic impact of QDs to DNA and its biological function.

2 Materials and methods

2.1 Chemicals

All chemicals were purchased from Sigma Aldrich (St. Louis, MA, USA) in ACS purity unless noted otherwise. Lyophilized highly polymerized DNA (Reanal, Hungary) was isolated from chicken erythrocytes ($M_w = 400\,000$ g/mol). The stock solution of DNA (1 mg/mL) was prepared by dissolving in ACS water.

2.2 DNA amplification and isolation

Taq PCR kit and DNA isolated from bacteriophage λ (48 502 bp) were purchased from New England BioLabs (USA). Primers for PCR were synthesized by Sigma-Aldrich. The sequence of a forward primer was 5'-CCTGCTCTGCCGCTTCACGC-3' and the sequence of a reverse primer was 5'-TCCGGATAAAAACGTCGATGACATTTGC-3'. Fifty microliters reaction mixture was composed of 5 μ L 10 \times standard *Taq* reaction buffer, 1 μ L of 10 μ M dNTP solution mix, 1 μ L of each primer (10 μ M), 0.25 μ L of 5 U/ μ L *Taq* DNA polymerase, 1 μ L of 0.5 μ g/ μ L λ DNA, and 40.75 μ L H₂O (sterile). The PCR tubes with mixture were placed into the cyclor (Eppendorf, Germany) and cycling conditions were as follows: initial denaturation at 95°C for 120 s; 25 cycles of denaturation at 95°C for 15 s, annealing at 64°C for 15 s, extension at 72°C for 45 s and a final extension at 72°C for 5 min. Hundred microliters of PCR product (500 bp) was purified by MinElute PCR Purification Kit (Qiagen, Germany) according to manufacturer's instruction and DNA was concentrated to 10 μ L of water solution. DNA concentration was determined by spectrophotometric analysis at 260 nm using spectrophotometer Specord 210 (AnalytikJena, Germany).

2.3 CdTe quantum dots synthesis

The procedure for synthesis of these dots was adapted from the work of Duan et al. [29]. Briefly, the synthesis of CdTe QDs and their subsequent coating were as follows: 4 mL of the CdCl₂ solution (0.04 M) was diluted with 42 mL of water. During constant stirring, 100 mg of sodium citrate, 4 mL of Na₂TeO₃ solution (0.01 M), 300 mg of reduced glutathione (GSH), and 50 mg of NaBH₄ were added into water-cadmium(II) solution. The mixture was kept at 95°C under the reflux cooling for 4 h. As a result, yellow solution of the GSH-QDs was obtained.

2.4 Spectroscopic and size analysis

Fluorescence and absorbance spectra were measured by multifunctional microplate reader Tecan Infinite 200 PRO 132 (TECAN, Männedorf, Switzerland). Excitation wavelength was 230 nm and emission range was measured from 300 to 850 nm per 5 nm steps. The absorbance was acquired within the range from 230 to 800 nm with 5 nm steps as an average of five measurements per well. The detector gain was set to 80. The sample volume of 50 μ L was placed in UV-transparent 96-well microplate with flat bottom by Costar (Corning, New York, USA). Zetasizer 3000 HSa (Malvern Instruments, Worcestershire, UK) was used for determination of size nanoparticles based on dynamic light scattering technique.

2.5 Capillary electrophoresis

Backman P/ACETM MDQ electrophoresis system (Brea, CA, USA) with laser-induced detector was used for CE measurements. Excitation wavelength was 488 nm (argon ion laser) and emission wavelength was 520 nm. An uncoated fused silica capillary was used with total length of 60.5 cm, effective length of 50 cm, and internal diameter 75 μ m. A 20 mM borate (pH 9.2) was used as BGE. Separation was carried out at 20 kV in positive polarity and sample was injected hydrodynamically for 20 s using 3.4 kPa.

2.6 Agarose gel electrophoresis

Agarose gel (2% v/v, high melt, medium fragments, Chemos CZ, Prague, Czech Republic) was prepared with 1 \times TAE buffer (40 mM Tris, 20 mM acetic acid, and 1 mM ethylenediaminetetraacetic acid). Five microliters of samples were prepared with 5% v/v bromophenol blue and 3% v/v glycerol and loaded into the gel. A 100 bp DNA ladder (New England Biolabs, Ipswich, MA, USA) was used to monitor the size of analyzed DNA. The electrophoresis was run at 60 V and 6°C for 160 min. The gel was stained in 100 mL of TAE buffer with 50 μ L of ethidium bromide for 20 min and visualized by UV transilluminator (312 nm). The intensity of fluorescence was quantified using Carestream molecular imaging software (Carestream, USA)

3 Results and discussion

3.1 Quantum dots characterization

QDs are known as size-dependent nanomaterials. The size is controllable during the synthesis process, which can give us a desired absorbance and emission spectra important for their further application. In this study of DNA interaction with QDs, desired 2 nm sized QDs were synthesized according to the method described elsewhere [29]. The size of the QDs and

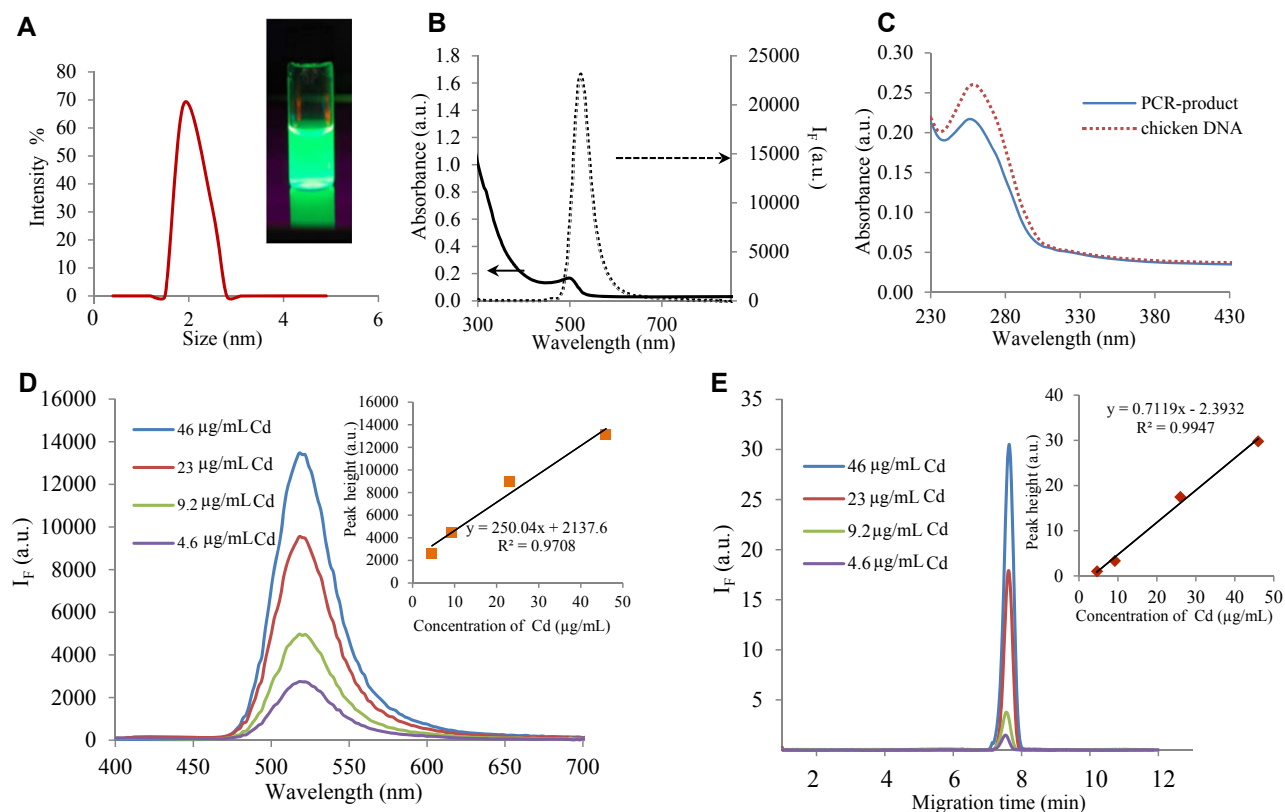


Figure 1. (A) Size determination of QDs by zeta-sizer, inset: photograph of QDs solution under UV light illumination. (B) Fluorescence and absorbance characterization of QDs. (C) Absorbance characterization of DNA and 500 bp fragment (200 µg/mL). (D) Fluorescence characterization of QDs diluted in water. All characterization was done by Tecan Infinite 200 PRO 132 under the following conditions: excitation wavelength was 230 nm and emission range was measured from 300 to 850 nm per 5 nm steps. The absorbance was acquired within the range from 230 to 1000 nm with 5 nm steps as an average of five measurements per well. Each intensity value is an average of five measurements. The detector gain was set to 80. The sample volume of 50 µL was placed in UV-transparent 96-well microplate with flat bottom by Costar. (E) CE characterization of QDs diluted in water. CE measurement is done by Beckman P/ACE™ MDQ electrophoresis system with LIF detector. Excitation wavelength was 488 nm and emission wavelength was 520 nm. An uncoated fused silica capillary was used with total length of 60.5 cm, effective length of 50 cm and internal diameter 75 µm. The 20 mM borate (pH 9.2) was used as BGE. Separation was carried out at 20 kV in positive polarity and sample was injected hydrodynamically for 20 s using 3.4 kPa. Concentration of QDs was recalculated to Cd concentration of 460 µg/mL according to [30].

their size-distribution is shown in Fig. 1A. The majority of the nanoparticles were 2 nm in diameter. The photograph of the solution of synthesized QDs under UV light illumination is shown in the inset in Fig. 1A exhibiting significant green light emission. Afterwards, their fluorescent properties were examined and their absorption maximum in visible range of spectra is 490 nm as indicated in Fig. 1B. The emission maximum after excitation by 490 nm light is at 525 nm. The absorption spectra of chicken genomic DNA and 498 bp fragment of bacteriophage λ used in the following experiments are shown in Fig. 1C.

To verify the linearity of the fluorescence signal depending on the concentration, the emission spectra of QDs were acquired (Fig. 1D). The concentration of QDs was expressed as the concentration of cadmium (inset in Fig. 1D). The Cd concentration in QDs was determined as described by Sobrova et al. [30]. The same characterization was performed by CE-LIF as shown in Fig. 1E. The peak of QDs with migration time of 7.5 min was observed and its height is lin-

early dependent on Cd concentration as shown in the inset in Fig. 1E.

3.2 CE-LIF analysis of interaction between DNA and quantum dots

After size and fluorescent characteristics of the QDs were verified, the interaction of these nanomaterials with DNA was studied. In the first experiment, the interaction between QDs and chicken genomic DNA was observed and results are shown in Fig. 2. The time dependence of complex formation can be seen in Fig. 2A. The peak 1 represents the DNA-QD complex and peak 2 represents the excess of the QDs. The increasing of the interaction time led to the increase of the peak 1 height. The dependence of the peak 1 height on time is shown in the inset in Fig. 2A. The same experiment measured by fluorescence spectroscopy exhibited only a very slight increase of the fluorescence intensity with the increasing time

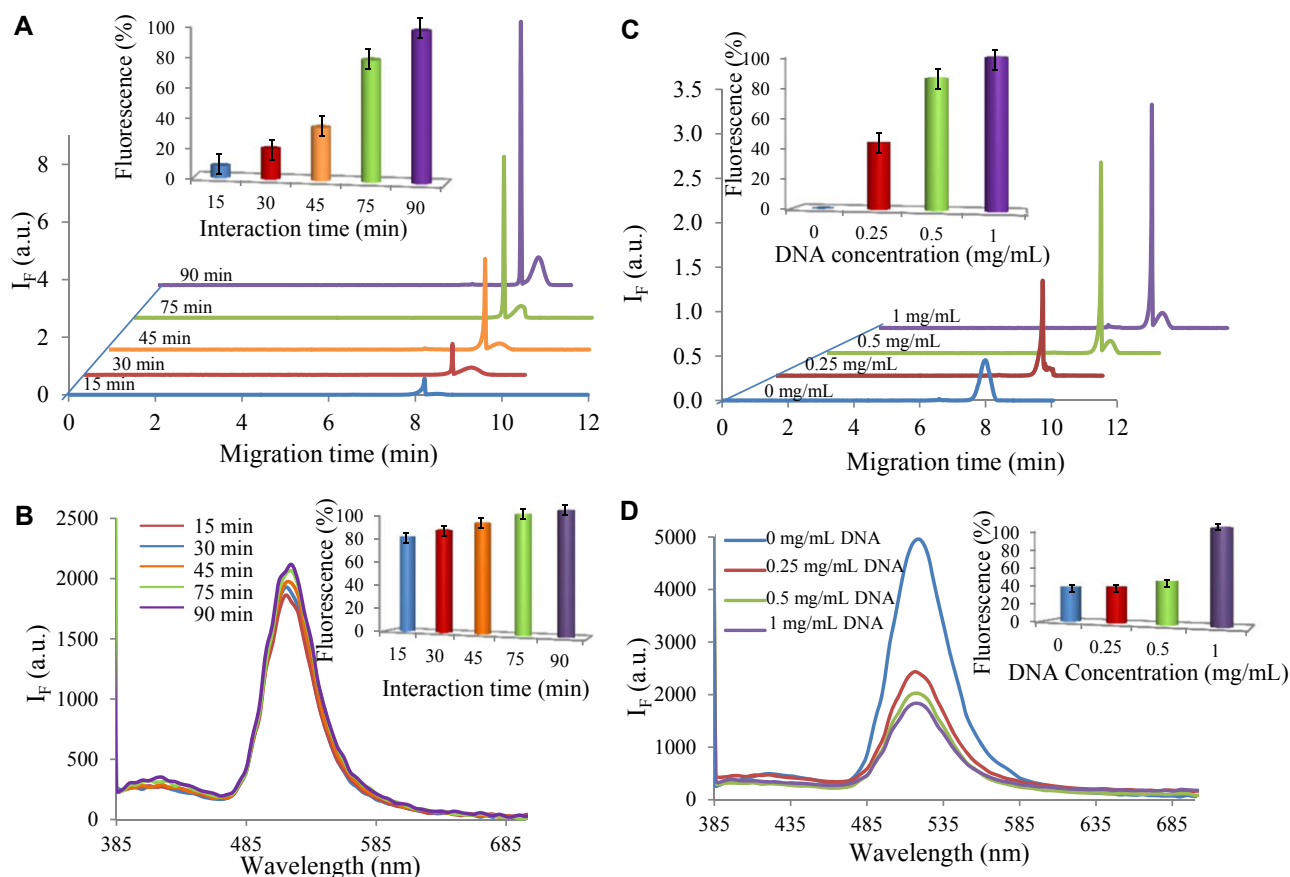


Figure 2. CE-LIF and fluorimetric characterization of QDs-DNA interaction. (A) QDs and DNA (500 $\mu\text{g}/\text{mL}$) time interaction (15, 30, 45, 75, and 90 min) monitored by CE-LIF, inset: the peak height dependence on time of interaction (peak 1 – QD-DNA complex, peak 2 – QDs). (B) QDs and DNA time interaction (15, 30, 45, 75, and 90 min) monitored by fluorescence spectrometry, inset: fluorescence intensity dependence on the interaction time. (C) QDs and DNA interaction with different concentrations of DNA (0, 0.25, 0.5, and 1 mg/mL) measured by CE-LIF, inset: dependence of created complex peak height on DNA concentration (peak 1 – QD-DNA complex, peak 2 – QDs). (D) QDs and DNA interaction with different concentrations of DNA (0, 0.25, 0.5, and 1 mg/mL) measured by fluorescence spectrometry, inset: fluorescence intensity dependence on the DNA concentration. CE and measurement with fluorimetric conditions are the same as in Fig. 1.

of interaction (Fig. 2B). The dependence of fluorescence intensities at 520 nm on the interaction time is shown in the inset in Fig. 2B. These results suggest that CE-LIF exhibits higher sensitivity for investigation of complex formation.

Subsequently, the dependence on DNA concentration was investigated. As it is shown in Fig. 2C, the increase in DNA concentration (from 0.25 to 1 mg/mL) led to the increase in peak height of the DNA-QD complex. Concentration dependence is shown in the inset in Fig. 2C. Using the fluorescence spectroscopy to verify the interaction, significant quenching effect of DNA on the QDs fluorescence was observed, however only a very small change of fluorescence was observed according to DNA concentration (Fig. 2D). In addition, the dependence of fluorescence intensities at 520 nm on the DNA concentration is shown in the inset in Fig. 2D.

The basic mechanism of interaction suggested in this study is based on the QDs incorporation into the major groove of DNA. The double-helical DNA structure creates major and

minor grooves with dimensions of 2.1 nm and 0.6 nm, respectively. Due to the matching size of QD (2 nm) to the size of major groove (2.1 nm) it can be suggested that the QD is incorporated into the major groove of DNA. This conclusion corresponds to previous work done by [31]. The scheme is shown in the inset in Fig. 3. To confirm this hypothesis, the interaction between QDs and ssDNA or dsDNA was monitored (Fig. 3). Results showed that dsDNA is needed for the complex (peak 1) to be created, while the complex is not observed with ssDNA.

Further, the interaction of QDs with 500 bp-long DNA fragment and as well as the influence of the DNA length was investigated. The 500 bp-long fragment induced formation of the QD-DNA complex in the same way as long DNA (Fig. 4). The complex formation (peak 1) with the increasing tendency depending on the interaction time was observed. The dependence of the peak height on the interaction time is shown in the inset in Fig. 4A. However, compared to the genomic DNA, the interaction of the fragment with QDs monitored by

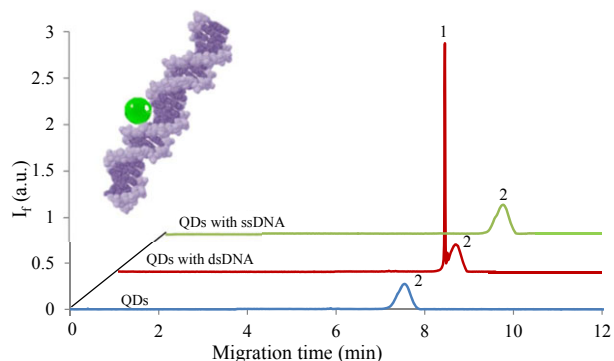


Figure 3. CE-LIF study of interaction between QDs (blue trace) and dsDNA (red trace, 500 $\mu\text{g}/\text{mL}$) or ssDNA (green trace, 500 $\mu\text{g}/\text{mL}$), (peak 1- QD-DNA complex, peak 2 – QDs), inset: the suggested scheme of the interaction between QD and major groove of dsDNA. Conditions of CE measurement are the same as in Fig. 1D.

fluorescence spectrometry did not exhibit the same increasing trend as observed by CE-LIF. Based on the comparison of the genomic DNA interaction to the DNA fragment interaction it can be assumed that the length of the DNA plays a key role especially due to the probability of the formation of numerous secondary structures. This has to be investigated in more details to reveal the impact of the DNA length on the interaction.

3.3 Gel electrophoresis

Gel electrophoresis was employed for DNA-QDs interaction verification. The gel after ethidium bromide staining is shown in Fig. 5A. The lines 1 and 13 were injected by the DNA ladder. The lines 2, 5, and 8 were injected with the QDs solution at concentration of 23, 46, and 460 $\mu\text{g}/\text{mL}$ mixed 1:1 with

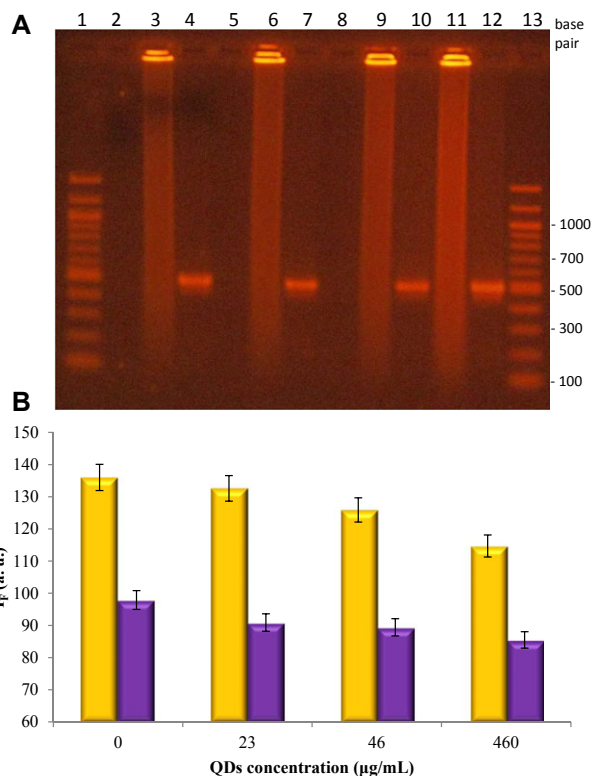


Figure 5. (A) Gel electrophoresis of the QD-DNA complex. (1) DNA Ladder, (2) QDs (230 $\mu\text{g}/\text{mL}$), (3) QDs 460 $\mu\text{g}/\text{mL}$ + chicken DNA (400 $\mu\text{g}/\text{mL}$) (1:1 v/v), (4) QDs (460 $\mu\text{g}/\text{mL}$) + 500 bp (50 $\mu\text{g}/\text{mL}$) (1:1 v/v); (5) QDs (23 $\mu\text{g}/\text{mL}$), (6) QDs 46 $\mu\text{g}/\text{mL}$ + DNA (400 $\mu\text{g}/\text{mL}$) (1:1 v/v), (7) QDs diluted 46 $\mu\text{g}/\text{mL}$ + 500 bp (50 $\mu\text{g}/\text{mL}$) (1:1 v/v), (8) QDs 11.5 $\mu\text{g}/\text{mL}$, (9) QDs 23 $\mu\text{g}/\text{mL}$ + DNA (400 $\mu\text{g}/\text{mL}$) (1:1 v/v), (10) QDs 23 $\mu\text{g}/\text{mL}$ + 500 bp (50 $\mu\text{g}/\text{mL}$) (1:1 v/v), (11) DNA (200 $\mu\text{g}/\text{mL}$), (12) 500 bp (25 $\mu\text{g}/\text{mL}$), (13) DNA ladder. For measurements 2% agarose gel in TAE buffer was used and run for 160 min at 60 V. Total amount of the samples was 10 μL . (B) Quenching of the signal dependent on the amount of QDs (chicken DNA–yellow columns, 500 bp DNA fragment–purple columns).

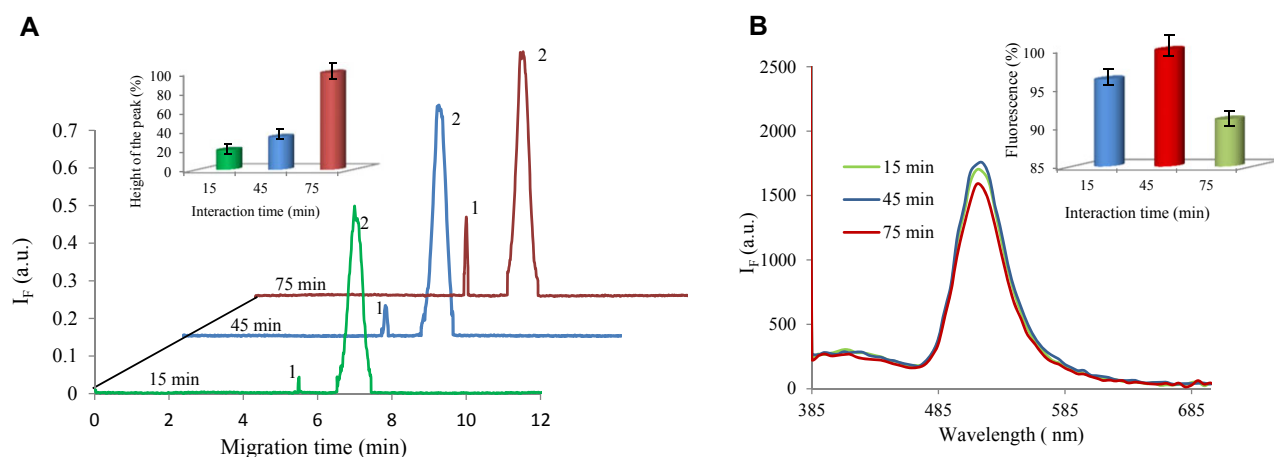


Figure 4. (A) CE-LIF and (B) fluorimetric characterization of the interaction between QDs (peak 2) and 500 bp long DNA fragment of bacteriophage λ (500 $\mu\text{g}/\text{mL}$). CE-LIF and fluorimetric measurement conditions are set as in the Fig. 1, inset: peak height dependence of QDs-DNA fragment complex on the reaction time.

water. In the lines 3, 6, and 9 there are the mixture samples of chicken DNA and 23, 46, and 460 $\mu\text{g}/\text{mL}$ of QDs in ratio 1:1, respectively. The same samples prepared using 500 bp DNA fragment and QDs are shown in the lines 4, 7, and 10. In lines 11 and 12, DNA and 500 bp fragment signal is observed. After software analysis of the gel image, the quenching of the signal dependent on the amount of QDs was observed for both chicken DNA as well as 500 bp fragment (Fig. 5B). This is probably due to the fact that QDs are preventing the DNA to be stained by the ethidium bromide.

4 Concluding remarks

It clearly follows from the results obtained that the interaction between DNA and QDs occurs. Monitoring and verification was successfully done by combination of CE-LIF and gel electrophoresis, whereas CE is analytical method with excellent separation characteristics and in the combination with LIF detector it provides very high selectivity needed for monitoring of DNA-QDs interaction. The obtained data confirm the hypothesis that the interaction mechanism is based on the size of QDs, which matches the size of DNA major groove.

The author M.V. wishes to express her thanks to project CZ.1.07/2.3.00/30.0039 for financial support. The author J.C. thanks to project GP 13-20303P.

The authors have declared no conflict of interest.

5 References

- [1] Adams, F. C., Barbante, C., *Spectroc. Acta Pt. B-Atom. Spectr.* 2013, *86*, 3–13.
- [2] Mattoussi, H., Palui, G., Na, H. B., *Adv. Drug Deliv. Rev.* 2012, *64*, 138–166.
- [3] Lacroix, L. M., Delpuch, F., Nayral, C., Lachaize, S., Chaudret, B., *Interface Focus* 2013, *3*, 1–19.
- [4] Acharya, A., *J. Nanosci. Nanotechnol.* 2013, *13*, 3753–3768.
- [5] Wang, Y. C., Hu, R., Lin, G. M., Roy, I., Yong, K. T., *ACS Appl. Mater. Interfaces* 2013, *5*, 2786–2799.
- [6] Byers, R. J., Hitchman, E. R., *Prog. Histochem. Cytochem.* 2011, *45*, 201–237.
- [7] Wu, H. F., Gopal, J., Abdelhamid, H. N., Hasan, N., *Proteomics* 2012, *12*, 2949–2961.
- [8] Fowler, B. A., Conner, E. A., Yamauchi, H., *Toxicol. Appl. Pharmacol.* 2008, *233*, 110–115.
- [9] Marko, N. F., Weil, R. J., Toms, S. A., *Expert Rev. Proteomics* 2007, *4*, 617–626.
- [10] Soman, C., Giorgio, T., *Nanomed.-Nanotechnol. Biol. Med.* 2009, *5*, 402–409.
- [11] Henry, M., Debarbieux, L., *Virology* 2012, *434*, 151–161.
- [12] Watson, J. D., Crick, F. H. C., *Cold Spring Harbor Symp. Quant. Biol.* 1953, *18*, 123–131.
- [13] Pang, D. W., Zhao, Y. D., Fang, P. F., Cheng, J. K., Chen, Y. Y., Qi, Y. P., Abruna, W. D., *J. Electroanal. Chem.* 2004, *567*, 339–349.
- [14] Mahtab, R., Sealey, S. M., Hunyadi, S. E., Kinard, B., Ray, T., Murphy, C. J., *J. Inorg. Biochem.* 2007, *101*, 559–564.
- [15] Sun, D. Z., Gang, O., *Langmuir* 2013, *29*, 7038–7046.
- [16] Zhang, C. L., Ji, X. H., Zhang, Y., Zhou, G. H., Ke, X. L., Wang, H. Z., Tinnfeld, P., He, Z. K., *Anal. Chem.* 2013, *85*, 5843–5849.
- [17] Pereira, M., Lai, E. P. C., Hollebhone, B., *Electrophoresis* 2007, *28*, 2874–2881.
- [18] Clarot, I., Wolpert, C., Morosini, V., Schneider, R., Balan, L., Diez, L., Leroy, P., *Curr. Nanosci.* 2009, *5*, 154–159.
- [19] Li, Y. Q., Wang, H. Q., Wang, J. H., Guan, L. Y., Liu, B. F., Zhao, Y. D., Chen, H., *Anal. Chim. Acta* 2009, *647*, 219–225.
- [20] Song, X. T., Li, L., Chan, H. F., Fang, N. H., Ren, J. C., *Electrophoresis* 2006, *27*, 1341–1346.
- [21] Stewart, D. T. R., Celiz, M. D., Vicente, G., Colon, L. A., Aga, D. S., *Trac-Trends Anal. Chem.* 2011, *30*, 113–122.
- [22] Wang, J. H., Li, Y. Q., Zhang, H. L., Wang, H. Q., Lin, S., Chen, J., Zhao, Y. D., Luo, Q. M., *Colloid Surf. A-Physicochem. Eng. Asp.* 2010, *364*, 82–86.
- [23] Akinfieva, O., Nabiev, I., Sukhanova, A., *Crit. Rev. Oncol./Hematol.* 2013, *86*, 1–14.
- [24] Wang, F. B., Rong, Y., Fang, M., Yuan, J. P., Peng, C. W., Liu, S. P., Li, Y., *Biomaterials* 2013, *34*, 3816–3827.
- [25] Stanisavljevic, M., Janu, L., Smerkova, K., Krizkova, S., Pizurova, N., Ryvolova, M., Adam, V., Hubalek, J., Kizek, R., *Chromatographia* 2013, *76*, 335–343.
- [26] Frigerio, C., Ribeiro, D. S. M., Rodrigues, S. S. M., Abreu, V. L. R. G., Barbosa, J. A. C., Prior, J. A. V., Marques, K. L., Santos, J. L. M., *Analytica Chimica Acta* 2012, *735*, 9–22.
- [27] Sang, F. M., Huang, X. Y., Ren, J. C., *Electrophoresis* 2014, *35*, 793–803.
- [28] Kuang, H., Zhao, Y., Ma, W., Xu, L. G., Wang, L. B., Xu, C. L., *Trac-Trends Anal. Chem.* 2011, *30*, 1620–1636.
- [29] Duan, J. L., Song, L. X., Zhan, J. H., *Nano Res.* 2009, *2*, 61–68.
- [30] Sobrova, P., Ryvolova, M., Hubalek, J., Adam, V., Kizek, R., *Int. J. Mol. Sci.* 2013, *14*, 13497–13510.
- [31] Xu, Q., Wang, J. H., Wang, Z., Yin, Z. H., Yang, Q., Zhao, Y. D., *Electrochem. Commun.* 2008, *10*, 1337–1339.